Desalination and Water Treatment
www.deswater.com

doi: 10.5004/dwt.2022.28266

252 (2022) 186–199
March

Comparative adsorption of Pb(II) on phosphoric acid- and sulfuric acid-modified lignocellulose-based cornstalk in aqueous solutions

Suksoon Choi[a], Hee-Jeong Choi[b,*]

[a]*Department of Biological and Environmental Engineering, Semyung University, 65, Semyung-ro, Jecheon, Chungcheongbuk-do, 27136, Republic of Korea, email: sschoi@semyung.ac.kr*
[a]*Department of Biosystems and Convergence Engineering, Catholic Kwandong University, Beomil-ro 579, Gangneung-Si, Gangwoon-do, 25601, Republic of Korea, Tel. +82 33 649 7297; Fax: + 82 33 647 7635; email: hjchoi@cku.ac.kr (ORCID: 000-0003-3370-4277)*

Received 19 August 2021; Accepted 29 January 2022

ABSTRACT

The purpose of this study was to compare and analyze the effects of phosphorylated (PCS) and sulfonated cornstalk (SCS) on the removal efficiency of cationic Pb(II) ions from aqueous solutions. The pH_{pzc} of cornstalk (CS) was 7.31, while those in SCS and PCS were lower at 4.17 and 2.25, respectively, confirming that acidic functional groups were attached to the surfaces of SCS and PCS. The maximum adsorption capacity of Pb(II) occurred in the order of PCS (182.76 mg/g) > SCS (114.36 mg/g) > CS (34.87 mg/g). The adsorption of Pb(II) onto SCS and PCS was close to chemisorption, and the adsorption efficiency increased in proportion to an increase in temperature. According to Fourier-transform infrared spectroscopy and Brunauer–Emmett–Teller analysis, sulfonation or phosphorylation of cornstalk help increased the number of carboxyl groups and porosity of the adsorbents, which facilitated the adsorbents to adsorb lead in aqueous solution. In summary, when CS was sulfonated and phosphorylated, the removal efficiency of Pb(II) from aqueous solutions was improved by 3.28 and 5.24 times, respectively.

Keywords: Adsorption; Cornstalk; Lead removal; Phosphorylation; Sulfonation

1. Introduction

Activated carbon has a large surface area, well-developed internal structure, and various surface functional groups, making it an excellent adsorbent for the removal of various contaminants [1]. However, due to the cost disadvantage of activated carbon, numerous approaches for the development of inexpensive and effective carbon adsorbents have been studied [2,3]. Agricultural waste is a suitable raw material for the production of high-quality activated carbon. Lignocellulose-derived biomass is a highly recommended source because it is readily available, low cost, and a regularly produced and renewable feedstock [4]. However, when various types of activated carbon were developed using biomass in a natural state without reforming, there were disadvantages in that the removal efficiency and regeneration of harmful substances was low [5]. Therefore, many researchers have been modifying lignocellulose-based biomass in various ways to increase the adsorption efficiency of harmful substances and to improve the regeneration of adsorbents [3,5].

Lignocellulose of biomass is a polymer in which cellulose, hemicellulose, and lignin are strongly crosslinked and bound through covalent or non-covalent bonds to form a lignocellulose matrix [6]. When lignocellulose biomass is modified, its specific surface area and pores are increased [7]. In addition, the surface of the adsorbent can be modified to be positively or negatively charged

* Corresponding author.

1944-3994/1944-3986 © 2022 Desalination Publications. All rights reserved.

depending on the modified material, thereby increasing its adsorption efficiency and selectiveness in adsorbing hazardous substances [7–9]. In particular, the lignocellulose-based biomass is composed of more than 90% carbon, and the chemical properties of the surface are hydrophobic [5]. Due to these properties, lignocellulose-based biomass is used as an adsorbent to remove heavy metals. For the material to adsorb harmful substances dissolved in water, water molecules adsorbed within the pores must be desorbed. When lignocellulose-based biomass is modified through chemical activation methods such as sulfuric acid and phosphoric acid, the dehydration effect that appears during the reforming process can suppress the formation of tar within the adsorbent [10,11]. The yield of porous carbon can be increased compared to that of the physical activation method, the activation time can be reduced, and a high degree of activation can be reached even at low temperatures [12,13].

The use of chemical activation reagents such as sulfuric acid, zinc chloride, potassium hydroxide, sodium hydroxide, and phosphoric acid has special activation strategies to improve the porosity and surface properties of activated carbon [7,13]. However, compared to other commonly used chemical activation reagents, phosphoric acid and sulfuric acid are advantageous due to their low activation temperature, high carbon yield, and generation of mesoporous structures [5,14]. The lower is the activation temperature, the larger is the number of acidic functional groups including carboxyl, phenolic hydroxyl groups, and lactones that can be retained on the surface of the lignocellulose-based adsorbent [8,13]. In addition, due to the phosphoric acid and sulfuric acid used during reforming, phosphorus or sulfur species can be introduced into the adsorbent to provide additional functional groups to further improve the adsorption of harmful substances [4,5]. In particular, phosphorus is an important group for adsorbing heavy metal ions in acidic solutions, and carbon activated by phosphoric acid can be a potential cation exchanger to remove harmful cationic substances from aqueous solutions [12,15]. Phosphoric acid can promote crosslinking through bond cleavage, cyclization, and condensation of biomass adsorbents in aqueous solutions [3,16]. These reactions form a bonding layer of material such as phosphate and polyphosphate that can protect the internal pore structure of the adsorbent, making it an excellent adsorbent in aqueous solutions [17]. According to previous studies, the adsorbent can be recycled and has various advantages such as low toxicity when modified by phosphoric acid [3,4,13,17]. New adsorbent materials with high adsorption capacity, fast adsorption rate, good reusability and cost-effectiveness are always welcome. Lignocellulose-based cornstalks are potential candidates for biosorbents of harmful substances, and the adsorption of harmful substances using cornstalks is valuable in that wastes are reused. Many studies [4,7,8,18] have been published on the adsorption of various heavy metals and dyes using cornstalks; however, there are limited studies on removal of Pb(II) through sulfonation and phosphorylation of cornstalks with a comparative analysis of removal efficiency. Therefore, in this study, cornstalk, a lignocellulose-based biomass, was modified and activated using sulfuric acid and phosphoric acid. The modified adsorbent was used to remove and compare the removal efficiency of Pb(II), one of the heavy metals with the greatest emission from aqueous solutions.

2. Materials and methods

2.1. Sulfonation and phosphorylation of cornstalk

Cornstalk (CS) samples were collected from areas grown without pesticides. Cornstalks were washed several times with tap water and then rinsed with distilled water to remove any contaminants attached to the surface. The washed CS were cut into small pieces and dried at 75°C ± 2°C for 24 h to remove moisture. The dried cornstalks were ground using an agricultural mill (SWISSMEX model Junior-r). Thereafter, the material with a particle size less than 40–60 mesh (0.25–0.4 mm) was recovered and sealed in a desiccator until use in the experiment.

Sulfuric acid (H_2SO_4) is a strongly acidic liquid compound that reacts with non-metals such as carbon to form sulfonic acid [9]. Sulfonation of CS using sulfuric acid was performed as follows. First, 20 g of cornstalk was added to 60 mL of ethyl alcohol cooled to –10°C and mixed well. After that, the mixture was added to 200 mL of cooled sulfuric acid, and sulfonation was carried out in a reactor (Yhana (Model SS-200, 50W)) while stirring at 150 rpm for 5 h so as not to exceed 10°C. The mixture was left at room temperature for 3 h for reaction completion. The adsorbent was washed several times with distilled water until the pH became neutral and was dried in a dryer for 48 h. Sulfonated cornstalks (SCS) were stored in a desiccator for use in experiments.

Phosphoric acid (H_3PO_4) is a type of inorganic oxygen acid and can refer to both the acid itself or the PO_4^{3-} ion [15]. Phosphoric acid in chemistry generally refers to an acidic reactant that contains phosphoric acid [12]. The method of activating cornstalk to porous carbon using phosphoric acid was as follows. First, 100 mL of 85% phosphoric acid and 75 g of phosphorus pentoxide were dissolved completely under heating and stirring. After cooling the solution, 20 g of cornstalk was added and phosphorylation was induced while stirring at 150 rpm for 5 h using a reaction device. The mixed sample was left at room temperature for 4 h to allow the reaction to occur completely; then, 1 N sodium hydroxide was added to adjust the pH to 7.5–8.0. Afterward the mixture was washed sufficiently with distilled water until the pH became neutral and was dried for 24 h in a dryer. The prepared phosphorylated cornstalks (PCS) were stored in a desiccator for use in experiments.

2.2. Experimental design

As Pb(II) was selected as the heavy metal solution, GR grade $Pb(NO_3)_2$ (Duksan Pure Chemicals, Co. Ltd., Korea, purity ≥99%) was used. Pb(II) was prepared at a concentration of 1,000 mg/L, diluted with distilled water, and used to prepare a solution of the required concentration. To investigate the effects of SCS and PCS on Pb(II) adsorption, various parameter experiments were carried out in the form of a batch test. A solution containing various concentrations of lead was placed into a 1 L Erlenmeyer flask, and an adsorbent was added according to the experimental plan to

observe the removal efficiency of lead onto PCS and SCS. The effects of various parameters on the removal efficiency of Pb(II) were tested while controlling various parameters such as pH (1–10), initial concentration of Pb (5–200 mg/L), contact time (0–240 min), and temperature (15°C–45°C). Sampling was performed at a predetermined time while stirring at 120 rpm in a shaking incubator.

2.3. Analytical methods

The collected samples were centrifuged at 1,500 rpm for 10 min and filtered using a 0.45 μm filter (Whatman filter), and the amount of Pb(II) was measured using atomic absorption spectrometry (AAS, PerkinElmer, AAS 3300, USA). The surface image of SCS and PCS was analyzed using scanning electron microscopy (SEM, JSM-IT500, JEOL Ltd., Japan) and Brunauer–Emmett–Teller (BET) surface area was examined using a BET Surface Analyzer (Quantachrome Instruments Version 11.03) via adsorption/desorption isotherms of N_2 performed at 77 k. The chemical compositions of CS, SCS, and PCS were analyzed using X-ray fluorescence (XRF, ZEISS Xradia 520, Germany) spectroscopy, and Fourier-transform infrared spectroscopy (FT-IR) was analyzed using a PerkinElmer Instrument (FT-IR 1760X, USA). The pH_{pzc} values of CS, SCS, and PCS were analyzed according to the method reported in a previous study [19]. All experiments were repeated five times, and the average value was used as the experimental result; to test one parameter, the other parameters were fixed. The pH was measured using a pH meter (SevenGO pro, Mettler Toledo). The adsorption kinetics were analyzed using pseudo-first-order (PFO) and pseudo-second-order (PSO) models, and the isothermal adsorption was analyzed using the Langmuir, Freundlich, and Temkin models; the thermodynamics were analyzed using Gibb's free energy equation. The various models used in the interpretation of the experimental results are summarized in Table 1.

To select the appropriate kinetic and isotherm models for the Pb(II) adsorption process, chi-squre (χ^2) was calculated using Eq. (1):

$$\chi^2 = \sum_{i=1}^{n} \frac{\left(q_{e,\exp} - q_{e,\mathrm{cal}}\right)^2}{q_{e,\mathrm{cal}}} \tag{1}$$

where $q_{e,\exp}$ and $q_{e,\mathrm{cal}}$ are the equilibrium adsorption capacity obtained from experiments and models, respectively.

3. Results and discussion

3.1. Characterization of adsorbents

3.1.1. Physical characteristics

The main component of CS is cell wall material, which accounts for about 67%–73% of lignocellulose; the cell content includes protein (7.1%), fat (1.0%), ash (8.4%), starch (3.2%), and pectin (2.3%) [20]. The component analysis results of CS, PCS, and SCS are summarized in Table 2. The main components of CS, PCS, and SCS were carbon and oxygen, though small amounts of hydrogen and nitrogen also were present. After sulfonation and phosphorylation of CS, the oxygen content increased and the carbon content decreased. This might have been due to the release of volatiles during sulfonation and phosphorylation processes; the relatively high oxygen content was thought to be due to the large amount of chemical active agents used.

As the H/C ratio approached 1, the aromaticity of the bioadsorbent increased; as the O/C ratio increased, the

Table 1
Adsorption kinetic, isotherm and thermodynamic models

Model	Equation	Parameters
Pseudo-first-order	$\ln\left(q_e - q_t\right) = \ln q_e - k_1 t$	q_t: amount of adsorbate adsorbed at time (mg/L); q_e: equilibrium adsorption capacity (mg/g); k_1: pseudo-first-order rate constant (1/min); t: time (min).
Pseudo-second-order	$\frac{t}{q_t} = \frac{1}{k_2 q_e^2} + \frac{t}{q_e}$	k_2: pseudo-second-order rate constant (L/mg min)
Langmuir	$\frac{1}{q_e} = \frac{1}{q_m K_L}\frac{1}{C_e} + \frac{1}{q_m}$ $R_L = \frac{1}{1 + K_L C_0}$	q_m: maximum adsorption capacity (mg/g); K_L: Langmuir constant (L/mg); C_e: equilibrium adsorbate concentration in solution (mg/L); C_0: initial adsorbate concentration in solution (mg/L); R_L: separation factor.
Freundlich	$\ln q_e = \ln K_F + \frac{1}{n}\ln C_e$	K_F: Freundlich constant (mg/g (L/mg)$^{1/n}$); n: heterogeneity factor.
Temkin	$q_e = B\ln K_T + B\ln C_e$	K_T: Temkin equilibrium binding constant (L/mg); B: Temkin constant (J/mol).
Gibbs free energy	$\Delta G° = \Delta H° - T\Delta S°$	$\Delta G°$: Gibbs free energy change (kJ/mol); $\Delta H°$: enthalpy change (kJ/mol); $\Delta S°$: entropy change (kJ/mol K).

anionic properties of the bioadsorbent were strengthened due to the increase in carboxylate groups on the surface of the adsorbent, which tended to increase the adsorption capacity of cationic substances [1,9]. After sulfonation and phosphorylation of CS, the H/C ratio improved from 0.04 to 0.12 and 0.15, respectively, and the ratio of O/C increased from 0.65 (CS) to 1.34 for SCS and 1.40 for PCS (Table 2). This showed that the carboxyl groups inside the adsorbents increased after phosphorylation and sulfonation of CS; the oxygen, hydrogen, and nitrogen contents increased after phosphorylation and sulfonation, indicating increased –OH and –NH groups in the adsorbent [9,12,15].

Ion exchange capacity refers to the ability of an adsorbent to adsorb harmful substances in an aqueous solution, expressed as the equivalent or weight of ions obtained by adsorbing a certain volume of the adsorbent [5,6,20]. According to previous studies, the ion exchange capacity was not necessarily proportional to the adsorption amount of harmful substances in an aqueous solution; however, the ion exchange capacity affected the adsorption quantity [4,17]. That is, when using the same adsorbent, when the ion exchange capacity was high, the adsorption amount increased; when the ion exchange capacity was low, the adsorption amount decreased [13,18]. As a result of phosphorylation and sulfonation of CS, the ion exchange capacity increased to 6.84 and 5.23, respectively, 4.2 and 3.2 times larger than that of CS, respectively.

Table 2
Characteristic of CS, PCS and SCS (unit: %)

Component (mass %)	CS	PCS	SCS
O	36.23	53.26	52.48
C	55.42	38.14	39.24
H	2.33	5.74	4.76
N	1.53	1.62	1.61
S	–	0.28	1.02
Mg	0.09	0.07	0.10
Surface property			
Pore volume (cm^3/g)	0.102	0.274	0.164
Pore diameter (nm)	0.835	5.32	4.28
BET surface area (m^2/g)	8.32	180.76	154.23
BET surface area (m^2/g) after adsorption	6.87	172.62	141.69
Ion exchange capacity (meq/g)	1.63	6.84	5.23

The results of BET measurement (Table 2) show the characteristics of CS, SCS and PCS. The surface area was significantly increased in PCS and SCS compared to CS. The activation process of PCS and SCS using phosphoric acid and sulfuric acid successfully enlarged the pores of CS. The high surface area of PCS provides sufficient active sites for Pb(II) adsorption. However, the surface area of PCS and SCS decreased after adsorption because Pb(II) ions were adsorbed on the PCS and SCS surface and covered the pores. Due to this, the pore volume of PCS and SCS was also reduced after Pb(II) adsorption.

The pore size of the adsorbent also could affect the adsorption efficiency. In general, sizes were divided into micropores (<2 nm), mesopores (2–50 nm), and macropores (>50 nm) [3,13]. According to a previous study, the adsorption efficiency of Pb(II) was highest in the micro-mesopore size than for super-micro ultra-fine pores (<1.0 nm) or macropores [15,21]. The pore sizes of PCS and SCS were 5.32 and 4.28, respectively, which corresponded to the range of macro-mesopores (Table 2).

3.1.2. Surface charge analysis

pH_{pzc} is an indicator of the adsorption range of adsorbent in an aqueous solution. In activated carbon, the surface of the adsorbent becomes positively charged at low pH centered on pH_{pzc} and is negatively charged at high pH [1,22]. Therefore, when cations are adsorbed, the lower is the pH_{pzc}, the wider is the range of adsorbable pH, which is advantageous for adsorption. In other words, at a pH above the isoelectric point, the surface of the adsorbent becomes negatively charged, and electrostatic interactions with the positively charged adsorbent material are strong, increasing adsorption efficiency. The pH_{pzc} of CS was 7.31 but decreased to 2.25 after phosphorylation and to 4.17 after sulfonation (Fig. 1). The acid group was attached strongly to the surface of PCS compared to SCS.

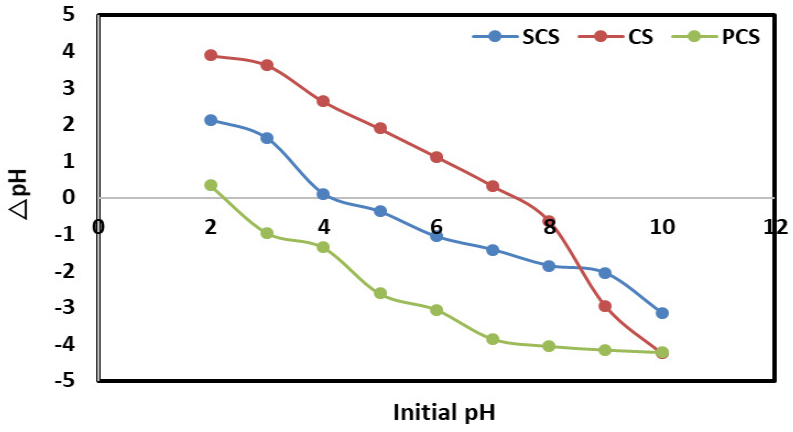

Fig. 1. The pH_{pzc} for CS, SCS and PCS in aqueous solution.

3.1.3. FT-IR spectra

The FT-IR spectra of PCS and SCS showed broadening and strengthening of certain bands according to modification of CS. The broad absorption band at 3,700–3,100 cm^{-1} is characteristic of hydrogen-bonded hydroxyl groups in carboxyl, phenol, or alcohol [2,3]. The FT-IR spectra showed a distinct peak at 1,600–1,650 cm^{-1} in all adsorbents of CS, SCS, and PCS (Fig. 2). This band was characteristic of the aromatic ring stretching mode enhanced by the presence of polar groups, indicating the presence of single or multiple aromatic rings in the structure of the carbon adsorbent [1,5]. All adsorbents also exhibited small peaks at 1,695–1,710 cm^{-1}, a characteristic of CO absorption in carboxylic acids. These low peaks were typical for carbon adsorbents and indicated bonding of CO with the aromatic ring system [1,13].

Phosphorylation introduced a phosphate group into CS, forming the widest OH group (3,100–3,700 cm^{-1}) and resulting in a deeper and wider 3,473 cm^{-1} peak. The 1,059 cm^{-1} peak represents ether, and that at 1,164–1,400 cm^{-1} corresponds to the $(RO)_3P{=}O$ peak [13,15]. The maximum peak of PCS was at 1,220–1,270 cm^{-1}; absorption in this region is found normally in oxidized carbon. This maximum peak was characteristic of phosphorus and phosphorus–carbon compounds present in phosphate-activated carbon, which appeared as the content of phosphocarbon compounds such as hydrogen bonds in phosphate or polyphosphate (such as P=O groups, P–O–C (aromatic) bonds, and P=OOH) increased due to phosphorylation [12,15,16]. Moreover, the small peaks at 1,070–1,090 cm^{-1} might have been due to symmetrical vibrations of P+O– in acidic phosphate ester and P–O–P of the polyphosphate chain [3,13].

SCS was bonded to OH-groups (3,000–3,500 cm^{-1}), CH stretching (2,900–2,800 cm^{-1}), and C=O carbonyl groups (1,740–1,680 cm^{-1}); and the peaks of carboxylic groups (1,670–1,640 cm^{-1}), CO stretch (1,450–1,300 cm^{-1}), C–O–C groups (1,200–1,230 cm^{-1}), SO_3H (1,150–1,165 cm^{-1}), and S=O group (1,010–1,040 cm^{-1}) were wide. In particular, the peak at 1,010–1,200 cm^{-1} was significantly broadened compared to that of CS because a sulfone group was introduced into this peak range.

The difference in FT-IR spectra of CS, SCS, and PCS was due to the influence of functional groups (sulfone or phosphate group). In addition, ether at 1,109 cm^{-1}, R–SO_3H absorption peak at 1,232 cm^{-1}, and ketone peaks at 1,642

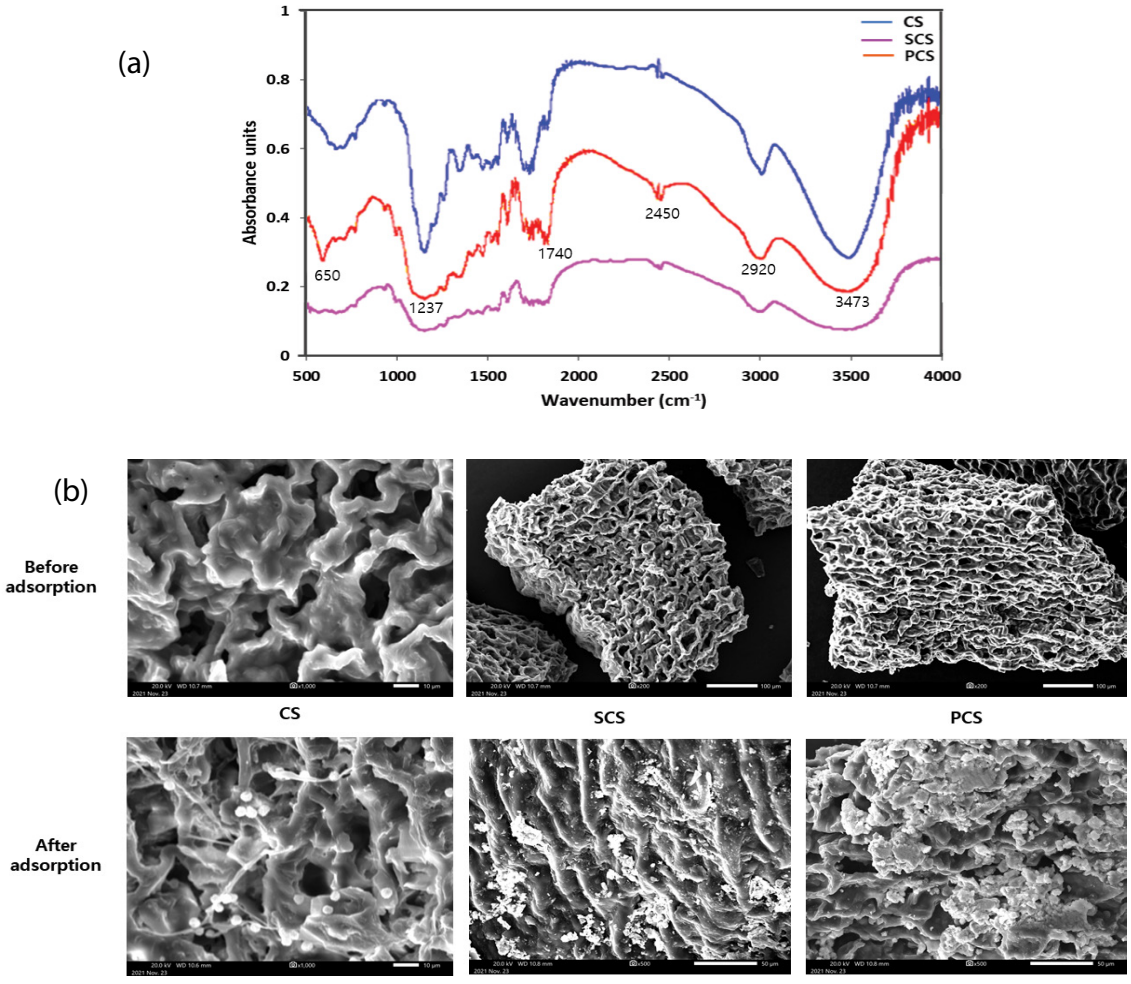

Fig. 2. FT-IR spectra (a) and SEM image (b) for CS, SCS and PCS.

and 1,477 cm^{-1} were confirmed to be sulfonated. In particular, the peak of N-containing bioligands (650 cm^{-1}), the R–SO_3H absorption peak (1,232 cm^{-1}), carboxylic groups (1,642 cm^{-1}), and bonded OH-groups (3,458 cm^{-1}) of SCS and PCS appeared wider than those in CS and had a larger number of functional groups. These indicate that the PCS and SCS adsorbents were changed to an easier structure for adsorption of Pb(II) compared to that of CS. Other than the surface area and porosity of the adsorbents, the presence of aromatic rings and functional groups such as –C=O, –COC–, –OH, –NH_2, –C=S, –C=N, –S=O, –P=O, –P–O–C, and P=OOH on the carbon surface played important roles in increasing the adsorption capacity of Pb(II) from aqueous solutions, which is in agreement with reports by the reference [1,3,5,16,17,20]. Changes in functional groups through phosphorylation and sulfonation are expected to affect the adsorption efficiency of Pb(II) in aqueous solutions.

The surface morphology of CS, SCS snd PCS was investigated by the SEM. Fig. 2b depicted a SEM image for before and after adsorption of Pb(II) by CS, SCS and PCS. Compared with CS, SCS and PCS were detected to have increased pores, with the rough surface while the size and shape were heterogeneously changed. This surface morphology provides a great advantage for adsorption because it can provide more adsorption sites for binding the adsorbate. In the SEM image after Pb(II) adsorption, it can be clearly confirmed that Pb(II) was adsorbed.

3.2. Parametric study

3.2.1. Dose of adsorbent

Being able to adsorb a large amount of harmful substances using a small amount of adsorbent in an aqueous solution is very economical because a small amount of adsorbent can be used, which is very helpful from an environmental aspect. The effects of CS, SCS, and PCS adsorbents on the adsorption efficiency of Pb(II) in aqueous solutions were observed. The experiment was conducted at a concentration of 0.1–2 g/L adsorbent, pH 7, and 25°C ± 1°C; the relationship between a lead removal efficiency greater than 90% and the adsorbent amount is depicted in Fig. 3.

The CS adsorbent and lead removal efficiency showed a correlation of 0.9954, and the lead removal efficiency was about 29.3 g/L using 1 g of adsorbent. On the other hand, the lead removal rate for SCS and PCS was determined to be 98.62 and 131.85 g/L, respectively, indicating 3.4 times and 4.5 times higher adsorption efficiency than CS. This result was because various functional groups, phosphoric acid groups, and sulfone groups were generated on the surface of the adsorbent through modification, which was consistent with the FT-IR analysis results of the adsorbent. As a result of Pb(II) adsorption in aqueous solutions using CS, SCS, and PCS, the largest amount of Pb(II) was adsorbed onto PCS followed by SCS. According to a previous study, when the adsorbent was sulfonated or phosphorylated, the ion exchange capacity was increased compared to the unmodified adsorbent; the Pb(II) removal efficiency was improved accordingly. As already mentioned in the introduction, this was in agreement with the results of many researchers who modified agricultural biomass to adsorb heavy metals in aqueous solutions.

3.2.2. pH

To examine the effect of pH on the adsorption efficiency of Pb(II), the pH was controlled from 1 to 10 by a 1 g/L adsorbent dose at 25°C ± 1°C. Pb(II) removal in aqueous solutions increased rapidly for CS from pH 7 and SCS from pH 4 (Fig. 4). Moreover, the removal efficiency of Pb(II) onto PCS increased rapidly from pH 2 to pH 5. However, the increase in removal efficiency was alleviated over pH 6 and was measured to be 126.35 mg/g at pH 6 and 133.53 mg/g at pH 10. This phenomenon was related to the value of pH_{pzc} mentioned above. This was because, when the pH was higher than pH_{pzc}, the surface of the adsorbent became negatively charged, making it easier to adsorb harmful cationic substances. In addition, as the pH increased, the sulfonic acid, carboxyl, and phenolic hydroxyl groups of the PCS and SCS adsorbents were deprotonated to form –P=O, –P–O–C, P=OOH, R–SO_3^{2-}, R–COO–, and R–O– groups. Due to this, the surfaces of the PCS and SCS adsorbents became negatively charged, improving the electrostatic

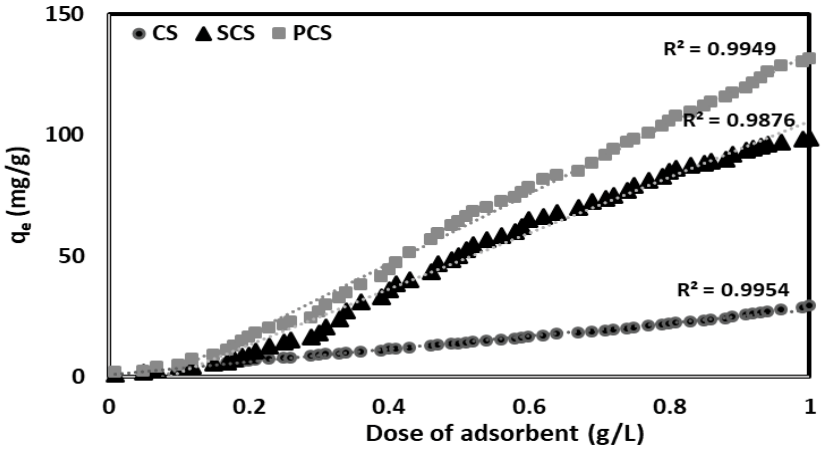

Fig. 3. Effect of various dose of CS, SCS and PCS for removal of Pb(II) (*V*: 1 L, pH: 7, mixing speed: 120 rpm, *T*: 298 K).

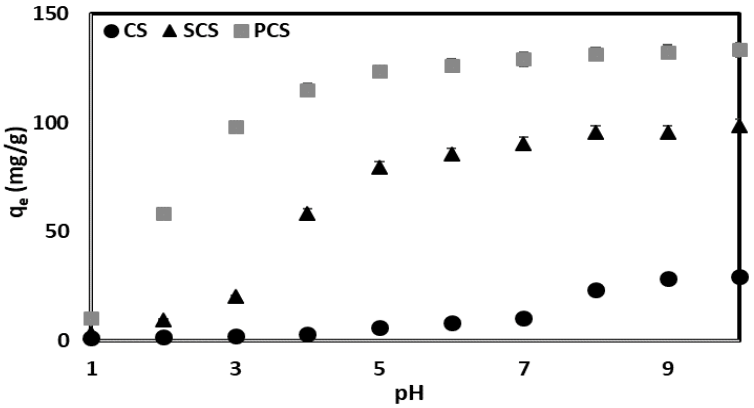

Fig. 4. Effect of various pH for removal of Pb(II) on CS, SCS and PCS (*C*: 150 mg/L, mixing speed: 120 rpm, *T*: 298 K).

attraction between PCS and SCS adsorbents and Pb(II) ions in aqueous solutions.

3.3. Adsorption kinetics and isotherms

3.3.1. Adsorption kinetics

To investigate the adsorption kinetics of CS, SCS, and PCS, PFO and PSO models were used for analysis. PFO relied on a monomolecular reaction, and PSO depended on the concentration of one secondary reactant or two primary reactants [1,22]. Therefore, when analyzing the adsorption kinetics of various adsorbents in aqueous solutions, it was often more suitable for PSO than PFO. The analysis results of the adsorption kinetics can be seen in Table 3 and Fig. 5.

As a result of the analysis of the adsorption kinetics, the $q_{e,\mathrm{cal}}$ of PSO was closer to the value of $q_{e,\mathrm{exp}}$ than that for PFO, and the correlation coefficient (R^2) of PSO was higher and χ^2 was lower than that for PFO in all of CS, SCS, and PCS. Therefore, the removal process of Pb(II) from aqueous solutions using CS, SCS, and PCS was more suitable for PSO than for PFO. In addition, the value of k_2 for PSO decreased as the concentration of Pb(II) increased in all three types of adsorbents. The adsorption rate of Pb(II) to the adsorbent decreased as the concentration of Pb(II) increased. This was because the higher was the concentration of Pb(II) in the aqueous solution, the lower was the active point that could be adsorbed to the adsorbent. In particular, PCS exhibited about 4 times higher adsorption efficiency than CS and 0.60–0.82 times higher than that of SCS. As already mentioned in the surface analysis of the adsorbent, it was closely related to the various functional groups on the adsorbent surface, the ion exchange capacity, and the pore size of the adsorbent.

3.3.2. Adsorption isotherm

In general, isothermal adsorption was analyzed using the Langmuir, Freundlich, and Temkin models. The Langmuir isothermal adsorption was a model created assuming that each reaction site had a uniform reaction intensity [5,13]. Freundlich's equation was an adsorption model created under the assumption that the adsorption sites of the adsorbent were not uniform, and the adsorption energy continuously decreased as the adsorption amount increased [17,23]. The Temkin isotherm showed that the heat of adsorption of Pb(II) ion decreased linearly rather than logarithmically with coverage [1,22]. The results of the isothermal adsorption experiment were analyzed using the Langmuir, Freundlich, and Temkin models and summarized in Table 4 and depicted in Fig. 6.

The dimensionless constant R_L (=1/(1 + $K_L C_0$), expressed as a separation coefficient or equilibrium coefficient calculated from Langmuir's equation, was calculated to be between 0.015–0.019, and the value of R_L was between 0 and 1. Thus, the use of CS, SCS, and PCS for adsorption of Pb(II) in aqueous solution was evaluated as suitable. The Temkin isothermal adsorption constant B was calculated to be 7.66 for CS, 22.32 for SCS, and 25.86 (J/mol) for PCS. Therefore, the adsorption of Pb(II) by CS was closer to physical adsorption caused by the action of van der Waals forces, which consisted of dispersion and electrostatic forces, than the chemical adsorption, in which the chemical form of the adsorbent was changed by a reaction between the adsorbent and adsorbent. However, the adsorption of Pb(II) by SCS and PCS were closer to chemisorption (B > 20 J/mol) than physical adsorption due to the change in the properties of the adsorbent by chemical substances. The K_F value, which indicated that the higher the value, the better the adsorption capacity, was the highest value at 45.62 for PCS, indicating that the adsorption capacity of Pb(II) in aqueous solutions was superior to that of CS or SCS. As for 1/n, the adsorption strength for CS, SCS, and PCS showed 0.077, 0.136, and 0.175, respectively; the PCS adsorbent had the highest adsorption strength. The R^2 value indicating the applicability of the adsorption model was greater than 0.99 in the Langmuir and Freundlich model for the adsorption of Pb(II) for both CS and SCS, however, the value of Langmuir was slightly higher than that of Freundlich. For PCS adsorbent, the R^2 value of the Langmuir model was significantly higher than the Freundlich model. Therefore, the adsorption of Pb(II) by CS, SCS, and PCS were best described by the Langmuir model. The maximum adsorption capacity of Langmuir was 34.87 mg/g for CS, 114.36 mg/g for SCS and 182.76 mg/g for PCS. In particular, PCS had a larger amount of Pb(II) adsorption than that

Table 3
Kinetics parameters for the adsorption of Pb(II) onto CS, SCS and PCS (amount of adsorbent: 1 g/L, pH: 7, *T*: 298 K)

Parameters		Concentration (mg/L)				
		50	100	150	200	300
CS						
$q_{e,exp}$ (mg/g)		10.62	18.34	23.21	28.26	32.57
Pseudo-first-order	$q_{e,cal}$ (mg/g)	9.22	16.76	19.97	25.14	28.43
	k_1	0.02	0.025	0.022	0.026	0.023
	R^2	0.9636	0.9684	0.981	0.9891	0.9884
	χ^2	2.9956	3.6896	4.7513	5.6985	6.2962
Pseudo-second-order	$q_{e,cal}$ (mg/g)	10.49	19.28	23.88	28.30	32.36
	$k_2 \times 10^{-4}$	6.59	1.20	0.65	0.36	0.25
	R^2	0.9894	0.983	0.9913	0.9894	0.9941
	χ^2	2.156	3.0396	3.5526	4.1459	4.6783
SCS						
$q_{e,exp}$ (mg/g)		38.53	59.91	76.24	93.26	113.22
Pseudo-first-order	$q_{e,cal}$ (mg/g)	34.43	50.07	65.43	79.62	93.76
	k_1	0.021	0.024	0.032	0.031	0.027
	R^2	0.952	0.9418	0.9456	0.9411	0.9748
	χ^2	2.9426	3.3257	4.4624	5.3596	5.9894
Pseudo-second-order	$q_{e,cal}$ (mg/g)	39.82	60.69	75.97	92.64	112.05
	$k_2 \times 10^{-6}$	14.71	3.87	1.82	1.0	0.59
	R^2	0.9924	0.9937	0.9886	0.9909	0.9958
	χ^2	1.9634	2.2462	3.1637	3.6785	4.2685
PSC						
$q_{e,exp}$ (mg/g)		47.23	98.67	128.46	157.25	178.63
Pseudo-first-order	$q_{e,cal}$ (mg/g)	47.41	76.52	88.29	101.34	123.09
	k_1	0.027	0.039	0.032	0.036	0.040
	R^2	0.9886	0.953	0.9043	0.8957	0.9287
	χ^2	2.4262	2.8463	3.5326	4.6215	5.0163
Pseudo-second-order	$q_{e,cal}$ (mg/g)	48.62	96.15	133.33	163.93	185.19
	$k_2 \times 10^{-6}$	8.47	1.13	0.42	0.23	0.16
	R^2	0.9937	0.9907	0.9968	0.997	0.9965
	χ^2	1.5632	2.1365	2.8951	3.3624	3.9657

of CS and SCS, because after modification with phosphoric acid the pores and functional groups were more developed. This was consistent with the above-mentioned FT-IR and BET analysis.

The experimental results of increasing the amount of lead adsorption in aqueous solutions by phosphorylation or sulfonation of bioadsorbents were in agreement with previous studies [10,15,17,24,25]. In particular, Hemavathy et al. [24] reported a remarkable increase in Pb(II) adsorption capacity from 13.22 to 129.3 mg/g in aqueous solutions as a result of sulfonation of *Cassia fistula* seeds. Jiang et al. [25] reported that phosphorylation of corn straw-converted hydrochar dramatically increased the adsorption capacity of Pb(II) from 32.7 to 353.4 mg/g. As seen in Table 5, when the biosorbent was phosphorylated and sulfonated, it was confirmed that the adsorption capacity of Pb(II) in aqueous solutions was significantly increased.

3.3.3. Interference of other ions

Various heavy metals exist together with lead in industrial wastewater, which may affect lead adsorption as an interfering substance. Therefore, Cd^{2+}, Cu^{2+}, Zn^{2+}, Mg^{2+}, Ni^{2+} and Cr^{3+}, which are generally present in industrial wastewater, were selected and the effect on adsorption of lead to SCS and PCS was investigated. Considering that the concentration of heavy metals in industrial wastewater is 20 mg/L or less, the experiment was carried out with 20 mg/L concentration of Cd, Cu, Zn, Mg, Ni, Cr and Pb, pH 7 and 1 g/L PCS or SCS at 25°C ± 1°C. As seen in Fig. 7, the adsorption efficiency of Pb(II) was found to be 100% in the presence of Cd, Cu, Zn, Mg, Ni, and Cr. This experimental data clearly confirms that other interfering ions did not affect the removal efficiency of lead. Specifically, the removal efficiency of divalent cations (Cd, Cu, Zn, Mg,

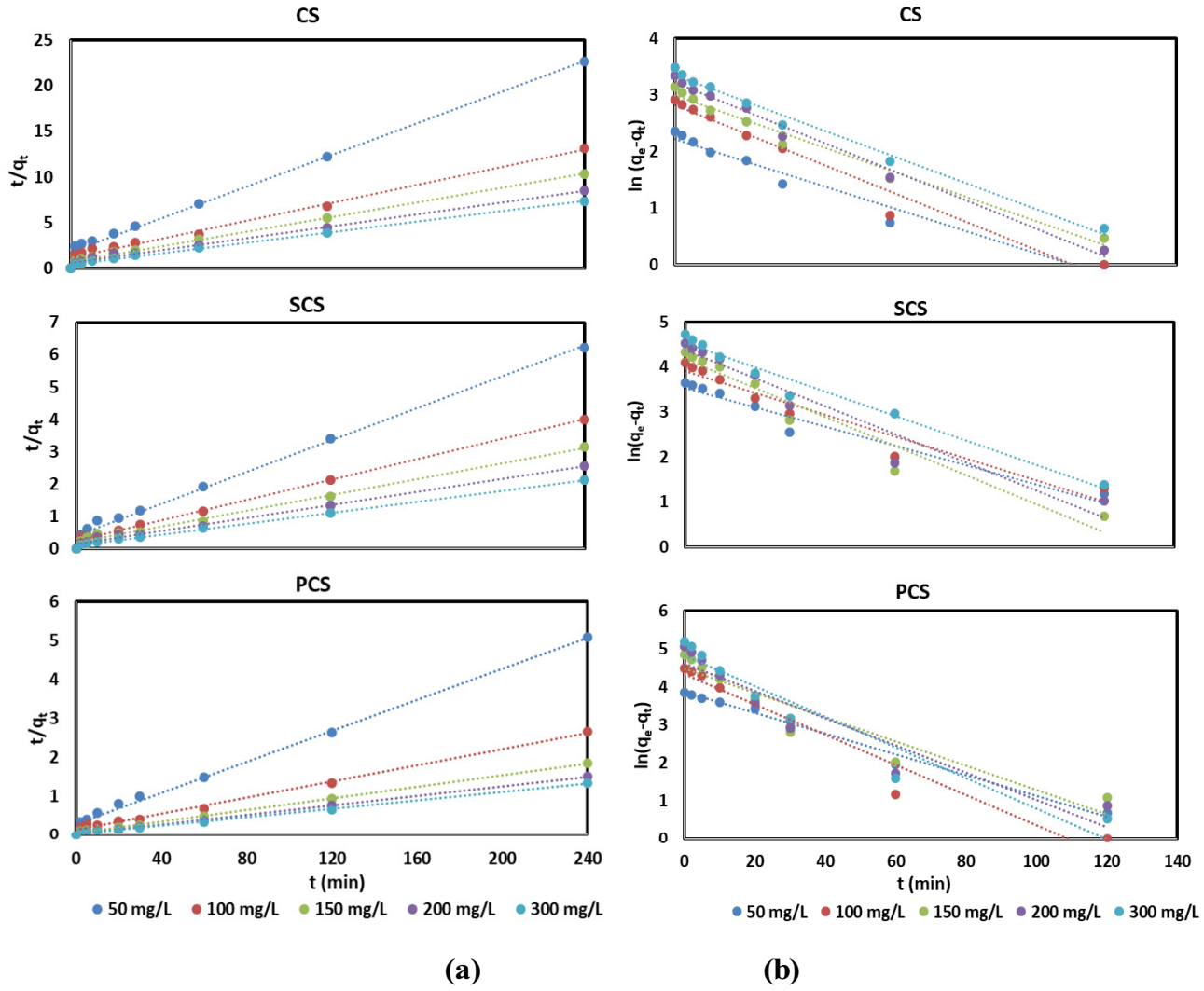

Fig. 5. Linear plot of (a) pseudo-first-order and (b) pseudo-second-order (*C*: 50–300 mg/L, mixing speed: 120 rpm, *T*: 298 K).

Table 4
Adsorption isotherms for Pb(II) on CS, SCS and PCS at 298 K

Isotherm	Parameters	CS	SCS	PCS
Langmuir	q_m (mg/g)	34.87	114.36	182.76
	K_L (L/mg)	2.62	3.13	3.41
	R^2	0.994	0.9972	0.999
	χ^2	2.1325	1.9263	1.5209
Freundlich	K_F ((mg/g)(L/mg)$^{1/n}$)	8.36	21.56	45.62
	$1/n$	0.077	0.136	0.175
	R^2	0.9923	0.9928	0.8245
	χ^2	4.0632	3.6514	2.8569
Temkin	B (J/mol)	7.66	22.32	25.86
	K_T (L/mg)	11.27	31.63	55.23
	R^2	0.4617	0.5219	0.6952
	χ^2	7.9632	5.6345	3.6594

Ni) was over 60% by both SCS and PCS, but the removal efficiency of trivalent cations (Cr) was very low (about 18%). These results indicate that SCS and PCS have a very high affinity for divalent cationic heavy metals.

3.4. Adsorption mechanism

SCS and PCS are strong acid resins that have an ion exchange capacity due to sulfuric acid and phosphoric acid functional groups [20,35]. According to the literature, strong acid resins adsorb almost all cations in aqueous solutions and exchange them with hydrogen ions [15]. Since this ion exchange process is reversible, resins can be regenerated using strong acids when the ion exchange capacity is exhausted [12]. In addition, strong acid ion exchange resins have a low pH_{pzc} so their application range is very wide.

Bioadsorption using biomass mainly consists of four main mechanisms: chemisorption, physisorption,

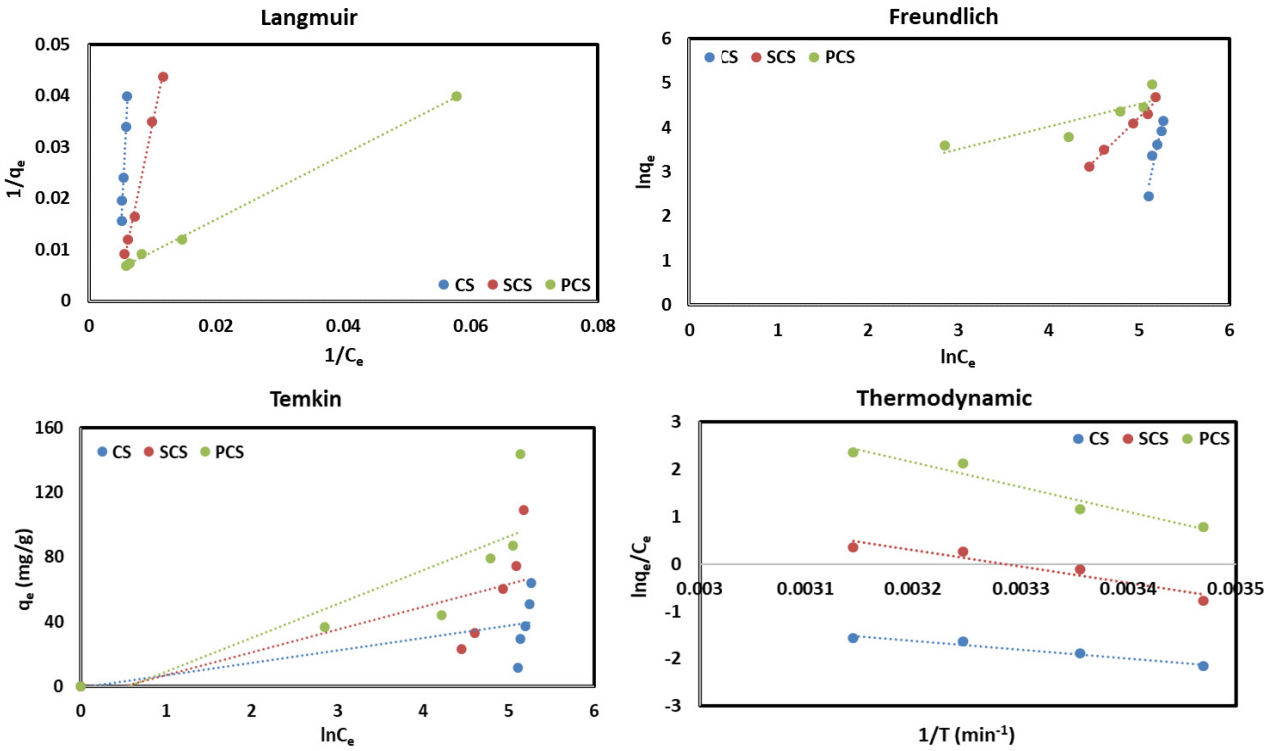

Fig. 6. A plot of Langmuir, Freundlich, Temkin and thermodynamic of Pb(II) onto CS, SCS and PCS.

Table 5
Comparison of SCS and PCS with other bioadsorbent to remove Pb(II)

Bioadsorbent	q_m (mg/g)	Reference
Persimmon leaves	22.59	[1]
Moringa oleifera bark	34.62	[26]
Coconut shell	26.14	[27]
Rice straw	42.55	[28]
Cassava peels	28.04	[5]
Groundnut shell	27.53	[5]
Yam peel	19.43	[5]
N,N′di(3-carboxysalicylidene)-3,4diamino-5-hydroxypyrazole onto mesoporous silica	169.34	[29]
4-tert-octyl-4-((phenyl)diazenyl)phenol onto inorganic mesoporous silica	200.80	[30]
Ti(IV) iodovanadate cation exchanger (TIV)	18.8	[31]
Corn straw-converted hydrochar	32.71	[25]
Modified oleifera bark	171.37	[32]
Cassia fistula seeds	13.22	[24]
Phosphoric acid modified sugarcane bagasse	73.75	[16]
Phosphoric acid activated bentonite	170.04	[33]
Phosphoric acid activated banana peels	241.03	[15]
Phosphoric acid activated corn straw-converted hydrochar	353.45	[25]
Sulfuric acid treated palm tree leaves	79.52	[25]
Sulfuric acid treated wheat bran	79.37	[34]
Sulfuric acid modified *Cassia fistula* seeds	129.32	[24]
Sulfuric acid modified cornstalk	114.36	This study
Phosphoric acid modified cornstalk	182.76	This study

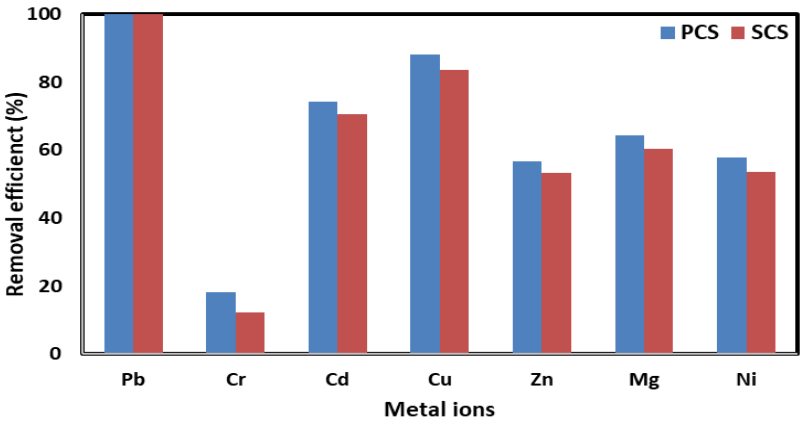

Fig. 7. Removal efficiency of Pb(II) with exist other ions by SCS and PCS.

microprecipitation, and oxidation/reduction [4,36]. Due to the complexity of the processes, more than one mechanism can occur simultaneously during bioadsorption [5]. Chemisorption consists of ion exchange, chelation, and complexation or coordination, while electrostatic interactions and van der Waals forces correspond to physisorption [12]. Various surface functional groups of the adsorbent play an important role in binding adsorbates during chemisorption. Ion exchange occurs through electrostatic interactions between negatively charged groups on the biomass surface and cations in solution [5,37]. Chelation refers to the formation of a ring structure due to the attachment of ligands and adsorbent ions [2,38]. The ring structure restricts attached minerals from entering undesirable chemical reactions [9,19]. Some biomass containing ligands has been reported to be beneficial to the chelation of Pb(II) [8,36,38]. Many researchers have suggested three possible models for the interaction between Pb(II) and sulfonated/phosphorylated adsorbents: electrostatic interactions, hydrogen bridge formation, and electron donor-acceptor relationships [11,16,35]. However, Hemavathy et al. [24] emphasized that the mechanism of Pb(II) adsorption on activated carbon is not fully controlled by electrostatic interactions, as evidenced by a positive effect of ionic strength on adsorption capacity. The change in ionic strength usually is due to the presence of intermolecular forces between adsorbent molecules and diffusion bilayer compression on the adsorbent surface [15,21,36]. The typical adsorption mechanism of Pb(II) on SCS and PCS in aqueous solutions can be explained through the following equations:

$$\text{R-OH} + \text{Pb}\left(\text{NO}_3\right)_2 \rightarrow \text{R-O-Pb} + \text{H}\left(\text{NO}_3\right)_2 \quad (2)$$

$$\text{R-NH}_2 + \text{Pb}\left(\text{NO}_3\right)_2 \rightarrow \text{R-N-Pb} + \text{H}_2\left(\text{NO}_3\right)_2 \quad (3)$$

$$\text{R-COOH} + \text{Pb}\left(\text{NO}_3\right)_2 \rightarrow \text{R-COO-Pb} + \text{H}\left(\text{NO}_3\right)_2 \quad (4)$$

$$\text{R-SO}_3\text{H} + \text{Pb}\left(\text{NO}_3\right)_2 \rightarrow \text{R-SO}_3\text{-Pb} + \text{H}\left(\text{NO}_3\right)_2 \quad (5)$$

$$\text{R-PO}_4\text{H} + \text{Pb}\left(\text{NO}_3\right)_2 \rightarrow \text{R-PO}_4\text{-Pb} + \text{H}\left(\text{NO}_3\right)_2 \quad (6)$$

FT-IR analysis showed that sulfonation and phosphorylation improved the number of carboxyls (–COOH) and hydroxyl groups, porosity, and the surface area of carbon. In particular, the formation of $–SO_3$ or $–PO_3$ groups on the surface of the adsorbent through the sulfonation or phosphorylation process is expected to play an important role during the adsorption of Pb(II) in aqueous solutions. As a result, the adsorption efficiency of Pb(II), a cationic ion, for SCS and PCS was improved.

3.5. Thermodynamic interpretation

In the adsorption process, reaction temperatures can affect all potential ion exchange materials as well as the solubility products of metal ions, which can determine the rate of adsorption. Since the solubility of metal ions can induce ion-exchange onto the adsorbent surface, it can affect the adsorption efficiency [39]. The effect of temperature on the adsorption efficiency in aqueous solutions was investigated, and the results are presented in Table 6.

The values of $\Delta H°$ and $\Delta S°$ are shown in Fig. 6, calculated from the slope and intercept of the van't Hoff plot ($\ln k_d$ vs. $1/T$). The value of $\Delta G°$ was value in CS and negative in SCS from a temperature of 308 K or higher. In particular, in the adsorption process by PCS, $\Delta G°$ showed a negative value, indicating spontaneous adsorption in nature. In addition, a positive $\Delta H°$ value indicated that the adsorption reaction was endothermic, and the adsorption efficiency increased as the temperature increased. A positive value of $\Delta S°$ indicated that the randomness of the adsorbent surface increased during the adsorption process. In particular, the $\Delta S°$ value increased in the order of CS, SCS, and PCS, and the randomness of the adsorbent surface increased in the order of CS < SCS < PCS. It was thought that, as the temperature increased, the kinetic energy of the molecules increased so molecular motion became active and entropy increased.

According to previous studies, opinions on the exothermic and endothermic reactions of the adsorption of harmful substances in aqueous solutions using lignocellulose-based

Table 6
Thermodynamic parameters for adsorption of Methylene blue on CS, SCS and PCS

Adsorbent	Temperature (K)	Thermodynamic [$\Delta G° = \Delta H° - T\Delta S°$]		
		$\Delta G°$ (kJ/mol)	$\Delta H°$ (kJ/mol)	$\Delta S°$ (J/mol K)
CS	288	5.10	15.80	37.14
	298	4.73		
	308	4.36		
	318	3.99		
SCS	288	1.55	28.78	94.55
	298	0.61		
	308	–0.34		
	318	–1.28		
PCS	288	–1.75	43.41	156.82
	298	–3.32		
	308	–4.89		
	318	–6.45		

biomass differ depending on the biomass used as the adsorbent [4,5]. Many researchers have reported that the bio-adsorption process was an endothermic reaction and that the adsorption efficiency was proportional to the increase in temperature [1,5,8,19,35]. This was because the number of available active sites increased as the temperature increased, and the adsorption efficiency increased due to the decrease in thickness of the boundary layer surrounding the adsorbent [2,22]. However, most researchers agree that bio-adsorbents using biomass can be denatured at high temperatures above 50°C, causing physical damage to adsorbents [3,15,17,23]. Therefore, to prevent denaturation of the adsorbent, it was recommended to refrain from performing the experiment at a temperature of 50°C or higher.

4. Conclusions

This study was intended to compare and analyze the removal efficiency of Pb(II) in aqueous solutions by phosphorylation and sulfonation of cornstalks. After phosphorylation and sulfonation of cornstalk, the adsorbent was changed to a structure that facilitated adsorption of Pb(II) in aqueous solutions due to changes in various functional groups on the adsorbent surface. In addition, the specific surface area, pore size, and ion exchange capacity were significantly increased in SCS and PCS. The pH_{pzc} of CS was 7.31 but was lowered to 4.17 in SCS and 2.25 in PCS, confirming that acidic functional groups were attached to the surfaces of SCS and PCS. The adsorption kinetics and isothermal adsorption test results of Pb(II) for CS, SCS, and PCS fit the PSO and Langmuir models. The maximum adsorption capacity was 34.87 mg/g for CS, 114.36 mg/g for SCS, and 182.76 mg/g for PCS. The adsorption process for SCS and PCS was close to chemisorption, and the higher was the temperature, the higher was the adsorption efficiency. Summarizing the experimental results, sulfonation and phosphorylation of CS could increase the adsorption efficiency of Pb(II) by 3.28 and 5.24 times in aqueous solutions, respectively.

Acknowledgement

This research was supported by Basic Science Research Program through the National Research Foundation of Korea (NRF) funded by the Ministry of Education (2021R111A305924311).

Compliance with ethical standards

The author(s) confirmed that this article content has no conflict of interest.

Declaration of competing interest

The authors declare that they have no known competing financial interests or personal relationships that could have appeared to influence the work reported in this paper.

CRediT authorship contribution statement

Hee-Jeong Choi (Prof. Ph.D): Conceptualization, Methodology, Data curation, Writing – original draft, Visualization, Investigation, Software, Validation, Writing – review and editing. Suksoon Choi: Conceptualization, Methodology, help in designing of methodology of this study.

Statement of informed consent, human/animal rights

No conflicts, informed consent, human or animal rights applicable.

References

[1] S.-Y. Lee, H.-J. Choi, Persimmon leaf bio-waste for adsorptive removal of heavy metals from aqueous solution, J. Environ. Manage., 209 (2018) 382–392.
[2] S.-W. Yu, H.-J. Choi, Application of hybrid bead, persimmon leaf and chitosan for the treatment of aqueous solution contaminated with toxic heavy metal ions, Water Sci. Technol., 78 (2018) 837–847.

[3] S. Basu, G. Ghosh, S. Saha, Adsorption characteristics of phosphoric acid induced activation of bio-carbon: equilibrium, kinetics, thermodynamics and batch adsorber design, Process Saf. Environ. Prot., 117 (2018) 125–142.
[4] Y. Dai, Q. Sun, W. Wang, L. Lu, M. Liu, J. Li, S. Yang, Y. Sun, K. Zhang, J. Xu, W. Zheng, Z. Hu, Y. Yang, Y. Gao, Y. Chen, X. Zhang, F. Gao, Y. Zhang, Utilizations of agricultural waste as adsorbent for the removal of contaminants: a review, Chemosphere, 211 (2018) 235–253.
[5] C.O. Thompson, A.O. Ndukwe, C.O. Asadu, Application of activated biomass waste as an adsorbent for the removal of lead(II) ion from wastewater, Emerging Contam., 6 (2020) 259–267.
[6] Y. Li, M. Wu, B. Wang, Y. Wu, M. Ma, X. Zhang, Synthesis of magnetic lignin-based hollow microspheres: a highly adsorptive and reusable adsorbent derived from renewable resources, ACS Sustainable Chem. Eng., 4 (2016) 5523–5532.
[7] N. Supanchaiyamat, K. Jetsrisuparb, J.T.N. Knijnenburg, D.C.W. Tsang, A.J. Hunt, Lignin materials for adsorption: current trend, perspectives and opportunities, Bioresour. Technol., 272 (2019) 570–581.
[8] S. Zhu, J. Xu, Y. Kuang, Z. Cheng, Q. Wu, J. Xie, B. Wang, W. Gao, J. Zeng, J. Li, K. Chen, Lignin-derived sulfonated porous carbon from cornstalk for efficient and selective removal of cationic dyes, Ind. Crops Prod., 159 (2021) 113071, doi: 10.1016/j.indcrop.2020.113071.
[9] G.A.O. Weijue, J.P.W. Inwood, P. Fatehi, Sulfonation of hydroxymethylated lignin and its application, J. Bioresour. Bioprod., 4 (2019) 80–88.
[10] A. Ämmälä, O. Laitinen, J.A. Sirviö, H. Liimatainen, Key role of mild sulfonation of pine sawdust in the production of lignin containing microfibrillated cellulose by ultrafine wet grinding, Ind. Crops Prod., 140 (2019) 111664, doi: 10.1016/j.indcrop.2019.111664.
[11] Y.-G. Park, K.-T. Kim, Selective separation of various heavy metals from synthesized phosphoric acid solutions, J. Ind. Eng. Chem., 95 (2021) 267–276.
[12] H. Zhuang, Y. Zhong, L. Yang, Adsorption equilibrium and kinetics studies of divalent manganese from phosphoric acid solution by using cationic exchange resin, Chin. J. Chem. Eng., 28 (2020) 2758–2770.
[13] N.V. Sych, S.I. Trofymenko, O.I. Poddubnaya, M.M. Tsyba, V.I. Sapsay, D.O. Klymchuk, A.M. Puziy, Porous structure and surface chemistry of phosphoric acid activated carbon from corncob, Appl. Surf. Sci., 261 (2012) 75–82.
[14] Q.-S. Liu, T. Zheng, P. Wang, L. Guo, Preparation and characterization of activated carbon from bamboo by microwave-induced phosphoric acid activation, Ind. Crops Prod., 31 (2010) 233–238.
[15] N. Zhou, H. Chen, Q. Feng, D. Yao, H. Chen, H. Wang, Z. Zhou, H. Li, Y. Tian, X. Lu, Effect of phosphoric acid on the surface properties and Pb(II) adsorption mechanisms of hydrochars prepared from fresh banana peels, J. Cleaner Prod., 165 (2017) 221–230.
[16] W.-l. Xiong, J. Zhang, J.-x. Yu, R.-a. Chi, Competitive adsorption behavior and mechanism for Pb^{2+} selective removal from aqueous solution on phosphoric acid modified sugarcane bagasse fixed-bed column, Process Saf. Environ. Prot., 124 (2019) 75–83.
[17] Q. Yang, P. Wu, J. Liu, S. Rehman, Z. Ahmed, B. Ruan, N. Zhu, Batch interaction of emerging tetracycline contaminant with novel phosphoric acid activated corn straw porous carbon: adsorption rate and nature of mechanism, Environ. Res., 181 (2020) 108899, doi: 10.1016/j.envres.2019.108899.
[18] A.H. Jawad, R.A. Rashid, M.A.M. Ishak, L.D. Wilson, Adsorption of methylene blue onto activated carbon developed from biomass waste by H_2SO_4 activation: kinetic, equilibrium and thermodynamic studies, Desal. Water Treat., 57 (2016) 25194–25206.
[19] H.E. Osman, R.K. Badwy, H.K. Ahmad, Usage of some agricultural by-products in the removal of some heavy metals from industrial wastewater, J. Phytol. Res., 2 (2010) 51–62.
[20] H.J. Choi, Surface modification of sulfuric acid-activated lignocellulose-based material for recovery of Ca, K, Mg, and Na from seawater, Desal. Water Treat., (2021), doi: 10.5004/dwt.2021.27525 (in Press).
[21] S. Pu, Z. Zhu, W. Song, H. Wang, W. Huo, J. Zhang, A novel acidic phosphoric-based geopolymer binder for lead solidification/stabilization, J. Hazard. Mater., 415 (2021) 125659, doi: 10.1016/j.jhazmat.2021.125659.
[22] H.-J. Choi, Assessment of the adsorption kinetics, equilibrium, and thermodynamic for Pb(II) removal using a low-cost hybrid biowaste adsorbent, eggshell/coffee ground/sericite, Water Environ. Res., 91 (2019) 1600–1612.
[23] J.C. Gómora-Hernández, M. del C. Carreño-de-León, N. Flores-Alamo, M. del C. Hernández-Berriel, S.M. Fernández-Valverde, Kinetic and thermodynamic study of corncob hydrolysis in phosphoric acid with a low yield of bacterial inhibitors, Biomass Bioenergy, 143 (2020) 105830, doi: 10.1016/j.biombioe.2020.105830.
[24] R.V. Hemavathy, A. Saravanan, P. Senthil Kumar, Dai-Viet N Vo, S. Karishma, S. Jeevanantham, Adsorptive removal of Pb(II) ions onto surface modified adsorbents derived from *Cassia fistula* seeds: optimization and modelling study, Chemosphere, 283 (2021) 131276, doi: 10.1016/j.chemosphere.2021.131276.
[25] Q. Jiang, W. Xie, S. Han, Y. Wang, Y. Zhang, Enhanced adsorption of Pb(II) onto modified hydrochar by polyethyleneimine or H_3PO_4: an analysis of surface property and interface mechanism, Colloids Surf., A, 583 (2019) 123962, doi: 10.1016/j.colsurfa.2019.123962.
[26] D. Harikishore Kumar Reddy, K. Seshaiah, A.V.R. Reddy, M. Madhava Rao, M.C. Wang, Biosorption of Pb^{2+} from aqueous solutions by *Moringa oleifera* bark: equilibrium and kinetic studies, J. Hazard. Mater., 174 (2010) 831–838.
[27] G.E. Sharaf El-Deen, S.E.A. Sharaf El-Deen, Kinetic and isotherm studies for adsorption of Pb(II) from aqueous solution onto coconut shell activated carbon, Desal. Water Treat., 57 (2016) 28910–28931.
[28] H. Amer, A. El-Gendy, S. El-Haggar, Removal of lead(II) from aqueous solutions using rice straw, Water Sci. Technol., 76 (2017) 1011–1021.
[29] A. Shahat, Md. Rabiul Awual, A. Khaleque, Z. Alam, Mu. Naushad, A.M. Sarwaruddin Chowdhury, Large-pore diameter nano-adsorbent and its application for rapid lead(II) detection and removal from aqueous media, Chem. Eng. J., 273 (2015) 286–295.
[30] Md. Rabiul Awual, Md. Munjur Hasan, A. Shahat, Functionalized novel mesoporous adsorbent for selective lead(II) ions monitoring and removal from wastewater, Sens. Actuators, B, 203 (2014) 854–863.
[31] Mu. Naushad, Z.A. ALOthman, Md. Rabiul Awual, Dr. Mohammad Mezbaul Alam, G. El-Baz El-Desoky, Adsorption kinetics, isotherms and thermodynamic studies for the adsorption of Pb^{2+} and Hg^{2+} metal ions from aqueous medium using Ti(IV) iodovanadate cation exchanger, Ionics, 21 (2015) 2237–2245.
[32] V.S. Munagapati, V. Yarramuthi, S.K. Nadavala, S.R. Alla, K. Abburi, Biosorption of Cu(II), Cd(II) and Pb(II) by *Acacia leucocephala* bark powder: kinetics, equilibrium and thermodynamics, Chem. Eng. J., 157 (2010) 357–365.
[33] M.F. Cheira, M.N. Rashed, A.E. Mohamed, G.M. Hussein, M.A. Awadallah, Removal of some harmful metal ions from wet-process phosphoric acid using murexide-reinforced activated bentonite, Mater. Today Chem., 14 (2019) 100176, doi: 10.1016/j.mtchem.2019.06.002.
[34] A. Özer, Removal of Pb(II) ions from aqueous solutions by sulphuric acid-treated wheat bran, J. Hazard. Mater., 141 (2007) 753–761.
[35] Y. Luo, X. Chen, Z. Zhao, X. Liu, J. Li, L. He, F. Sun, Pressure leaching of wolframite using a sulfuric-phosphoric acid mixture, Miner. Eng., 169 (2021) 106941, doi: 10.1016/j.mineng.2021.106941.
[36] A.M. Soliman, H.M. Elwy, T. Thiemann, Y. Majedi, F.T. Labata, N.A.F. Al-Rawashdeh, Removal of Pb(II) ions from aqueous

solutions by sulphuric acid-treated palm tree leaves, J. Taiwan Inst. Chem. Eng., 58 (2016) 246–273.
[37] H. Zeng, H. Zeng, H. Zhang, A. Shahab, K. Zhang, Y. Lu, I. Nabi, F. Naseem, H. Ullah, Efficient adsorption of Cr(VI) from aqueous environments by phosphoric acid activated eucalyptus biochar, J. Cleaner Prod., 286 (2021) 124964, doi: 10.1016/j.jclepro.2020.124964.
[38] J. Wolska, J. Walkowiak-Kulikowska, On the sulfonation of fluorinated aromatic polymers: synthesis, characterization and effect of fluorinated side groups on sulfonation degree, Eur. Polym. J., 129 (2020) 109635, doi: 10.1016/j.eurpolymj.2020.109635.
[39] X. Leng, Y. Zhong, D. Xu, X. Wang, L. Yang, Mechanism and kinetics study on removal of iron from phosphoric acid by cation exchange resin, Chin. J. Chem. Eng., 27 (2019) 1050–1057.